

# Multistability in platelets and their response to gold nanoparticles

Suryyani Deb, MSc<sup>a</sup>, Hirak K. Patra, MSc<sup>a</sup>, Prabir Lahiri, PhD<sup>a</sup>, Anjan Kr. Dasgupta, PhD<sup>a,\*</sup>,  
Kuntal Chakrabarti, PhD<sup>b</sup>, Utpal Chaudhuri, MD<sup>c</sup>

<sup>a</sup>Department of Biochemistry, University of Calcutta, Kolkata, India

<sup>b</sup>Department of Materials Science, S.N.Bose National Centre for Basic Sciences, Salt Lake, Kolkata, India

<sup>c</sup>Institute of Hematology and Transfusion Medicine, Calcutta Medical College, Kolkata, India

Received 25 June 2010; accepted 16 January 2011

## Abstract

The nanoparticle (NP) response of platelets is shown to be critically dependent on extent of preactivation of platelets by an agonist like ADP. A transition from de-aggregatory to aggregatory state is triggered in the presence of gold NPs (AuNP) only in such critical conditions. Adhered and suspended platelets respond differentially to NPs. Preactivation in the adhered state induced by shear force explains such observation. The NP effect is associated with enhanced release reaction, tyrosine phosphorylation and CD62P expression level. Unlike cancer cells, whose response is maximal when NP size is optimal (within the range 50–70 nm), the platelet response monotonically increases with reduction of the AuNP size. The uptake study, using quenching of quinacrine hydrochloride fluorescence by AuNP, indicates that accumulation 18 nm AuNP is several-fold higher than the 68 nm AuNP. It is further shown that AuNP response can provide a simple measure for thrombotic risk associated with nano-drugs.

**From the Clinical Editor:** Platelet aggregation can be triggered in the presence of gold nanoparticles (AuNP). Platelet response monotonically increases with reduction of the AuNP size. AuNP response can provide a simple measure for thrombotic risk associated with nano-drugs.

© 2011 Elsevier Inc. All rights reserved.

**Key words:** Gold nanoparticle; Multi-stability; Granule release; Adhesion; Activation; Nanosafety measure; Thrombotic risk

The last few years have witnessed either an overly optimistic or an overly cautious approach in dealing with nanoparticle (NP) effects in drug delivery and diagnostics.<sup>1,2</sup> Although a few papers showed the promise of nano-based drug-delivery systems or of MRI contrast agents, a few were concerned with the adverse toxicological effects of such NPs.<sup>3–5</sup> Many of the drugs in question have to be administered through the vascular pathway. The interaction of nano-conjugated drugs may be subjected to direct exposure of the vascular components to the bare surface of the NP.

In this context, a deeper study of platelet NP interaction is required, as platelets play the most important role in hemostasis.<sup>6</sup> Platelet activation is inhibited by a number of physiological agents like nitric oxide, endothelial-ADPase, and PGI<sub>2</sub>.<sup>7</sup> When vessel injury occurs in collagen, von Willebrand Factor (vWF) and tissue factor from the sub-endothelial extra

cellular matrix (ECM) are exposed to the bloodstream and have a chance to activate platelets.<sup>7</sup> This activation also depends on the shearing force in the vessel.<sup>8</sup> It is widely accepted that platelets play a pivotal role in the development of cardiovascular disease<sup>9</sup> and consequently, the inhibitors of platelet aggregation (antiplatelet agents) have become essential components for the prevention of such disease.<sup>10</sup> Therefore, how and when a NP would interfere with the vascular pathway should therefore be considered as an integral part of the management of cardiovascular disease.

Our group was the first to report that metallic NPs can induce platelet aggregation,<sup>11</sup> which is supported by other researchers.<sup>3,12</sup> The carbon NP-induced pro-aggregatory response was initially reported by Radomski.<sup>13</sup> Both carbon nanotubes (CNTs) and metallic NPs caused aggregatory responses; however, they differed in their modes of action. The CNTs, which are strongly hydrophobic in nature,<sup>14</sup> cause aggregation in the absence of additional activation. The implication of this study is important, because CNTs and other hydrophobic noncolloidal NPs can be excluded from the list of possible future drug-delivery agents, provided special measures are taken to minimize their toxic effects. We earlier reported that metallic NPs could induce platelet aggregation

Funding Source: DBT, Govt. of India. (Grant No. BT/PR9953/MNT/28/73/2007).

\*Corresponding author: Department of Biochemistry, University of Calcutta, 35 Ballygunge Circular Road, Kolkata 700019, India.

E-mail address: [adgcal@gmail.com](mailto:adgcal@gmail.com) (A.K. Dasgupta).

1549-9634/\$ – see front matter © 2011 Elsevier Inc. All rights reserved.  
doi:10.1016/j.nano.2011.01.007

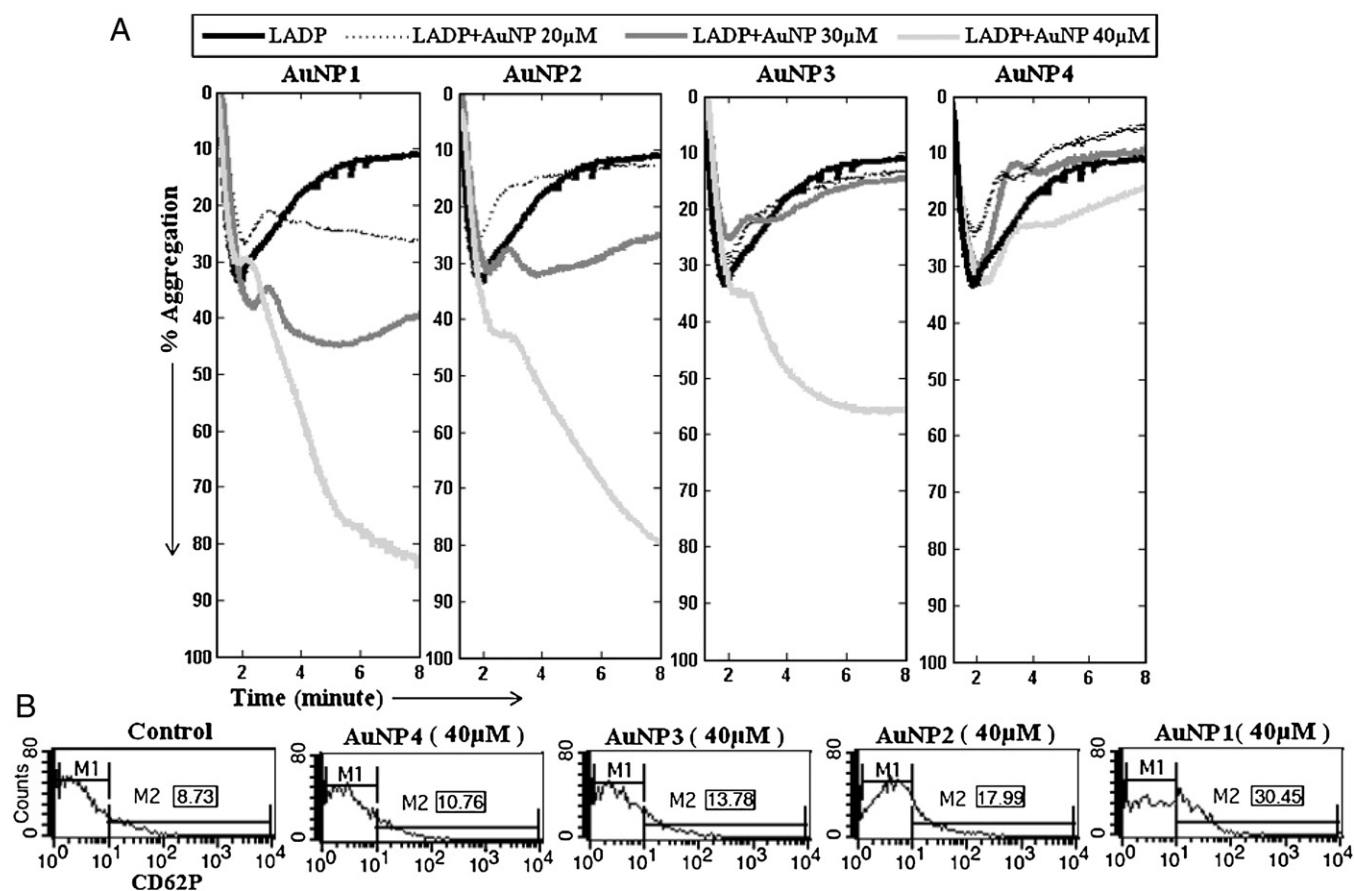


Figure 1. Size dependence and dose dependence of AuNPs. **(A)** Represents the dose dependence and size dependence of different AuNPs. The concentration of AuNPs increases from 20  $\mu\text{M}$  to 40  $\mu\text{M}$ , and the effect is maximum with the AuNP of 40  $\mu\text{M}$ . **(B)** represents the platelet activation profile, expression of surface CD62P level with the 40  $\mu\text{M}$  concentration of different AuNPs with the increasing order of size. In the release reaction study by flow cytometry M1 and M2 represent gated population percentage showing basal and higher level of CD62P expression.

only if a critical agonist dose is present.<sup>11</sup> Such threshold level preactivation may be an important consideration in the general nanomedicine context.

Gold NPs (AuNPs) are considered to be one of the safest drug-delivery agents usable in several drug-delivery contexts and also in hyperthermic treatment of cancer due to their inert property.<sup>2,15–16</sup> This article critically analyzes this safety aspect of AuNPs, which have a good record of killing cancer cells and nontoxic to normal cells.<sup>1</sup> Last, the question about whether the size at which AuNPs are most effective to kill cancer cells<sup>17</sup> is safe in a platelet context is also addressed in this article.

## Methods

The details of AuNP preparation, and their characterization by optical measurement, transmission electron microscopy (TEM)<sup>11,18</sup> is described in the Methods section of the [Supplementary Section](#). Similarly, the [Supplementary Section](#) describes the details of platelet aggregometry by conventional aggregometer as well as by the cone and plate technique.<sup>19–23</sup> The section also details the release reaction.<sup>20</sup> The washing of platelets for flow cytometric studies is also described.<sup>24,26</sup> The

immunoblotting study<sup>25</sup> is also detailed in the [Supplementary Section](#), which also contains the fluorescence of quenching of quinacrine hydrochloride (Q) by AuNP and the subsequent fluorescence imaging in the presence and absence of AuNP that is backed up by image-analysis studies. The Methods section in the [Supplementary Section](#) further details the platelet inhibition by Arg-Gly-Asp-Ser (RGDS) and the details of the methods followed in the statistical analysis of the results.

## Results

### Size dependence and dose dependence of AuNPs

Figure 1 summarizes the aggregometric and flow cytometric studies on platelets in presence of AuNP(s) of different sizes. The aggregation decreases with the increasing size and decreasing concentration of AuNP (Figure 1, A). The smaller size of AuNP (~20 nm) with 40  $\mu\text{M}$  final concentration exerts the maximal effect on platelets whereas the larger AuNP (~70 nm) remains almost neutral even at higher concentration. Figure 1, B shows that the expression of the surface CD62P is higher for the smaller AuNP. The M2 population (explained in

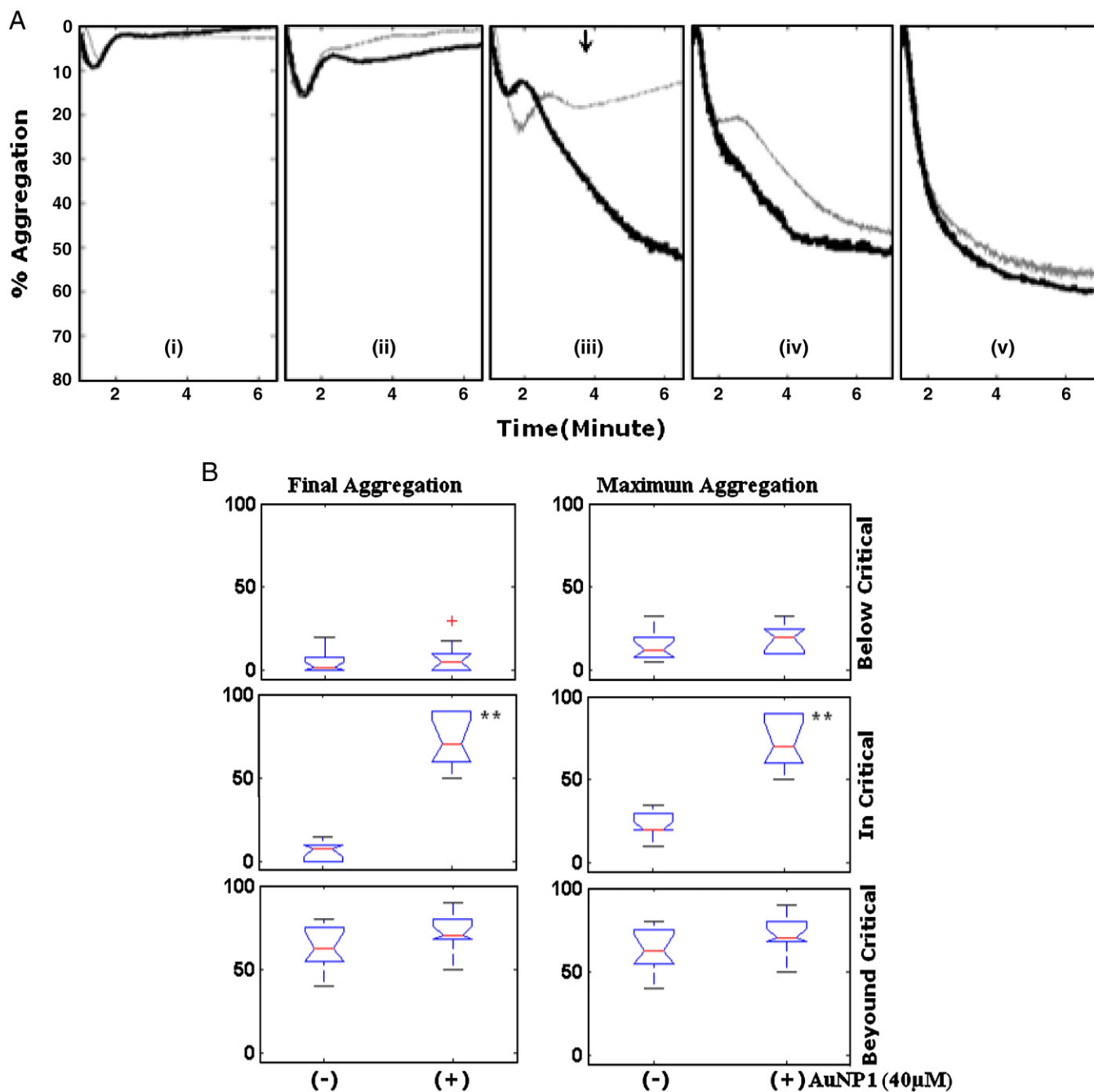


Figure 2. Critical ADP dependence of AuNP-induced platelet aggregation. **(A)** The lighter color represents the ADP induced aggregation alone, whereas the darker line represents the corresponding AuNP induced aggregation. Panel **(i)**, **(ii)**, **(iii)**, **(iv)**, and **(v)** represent platelet aggregation profile of respective ADP concentration 0.8 μM, 1.2 μM, 1.6 μM, 5.0 μM, 10.0 μM alone and with AuNP (~20 nm, 40 μM gold concentration) in each case. **(B)** Represents the difference in AuNP (40 μM) induced maximum aggregation and final aggregation in different conditions (below, in and beyond the critical concentration of ADP), by box plot. The critical ADP concentration has a range 1.5–2 μM. On the higher side, the typical ADP concentration being used is 5–10 μM. The symbol “\*\*” implies that  $P$  value < 0.01.

the figure legend) gradually increases with decreasing NP size. For control, the relative M2 population is ~8.73 %, whereas for AuNP4 (~70 nm), AuNP3 (~55 nm), AuNP2 (~45 nm) and AuNP1 (~20 nm) the M2 population becomes 10.8%, 13.7%, 17.9% and 30.4%, respectively. Again, the mean fluorescence of CD62P also increases with the decrease in AuNP size. For the control, the value of the mean fluorescence

is ~4.33% and for AuNP4, AuNP3, AuNP2 and AuNP1, it increases to 4.76%, 5.75%, 7.58%, and 10.02%, respectively.

#### Multistability of platelet behavior and AuNP response

The ADP-dependent alteration in the platelet aggregation profile and the critical nature of AuNP (~20 nm diameter and

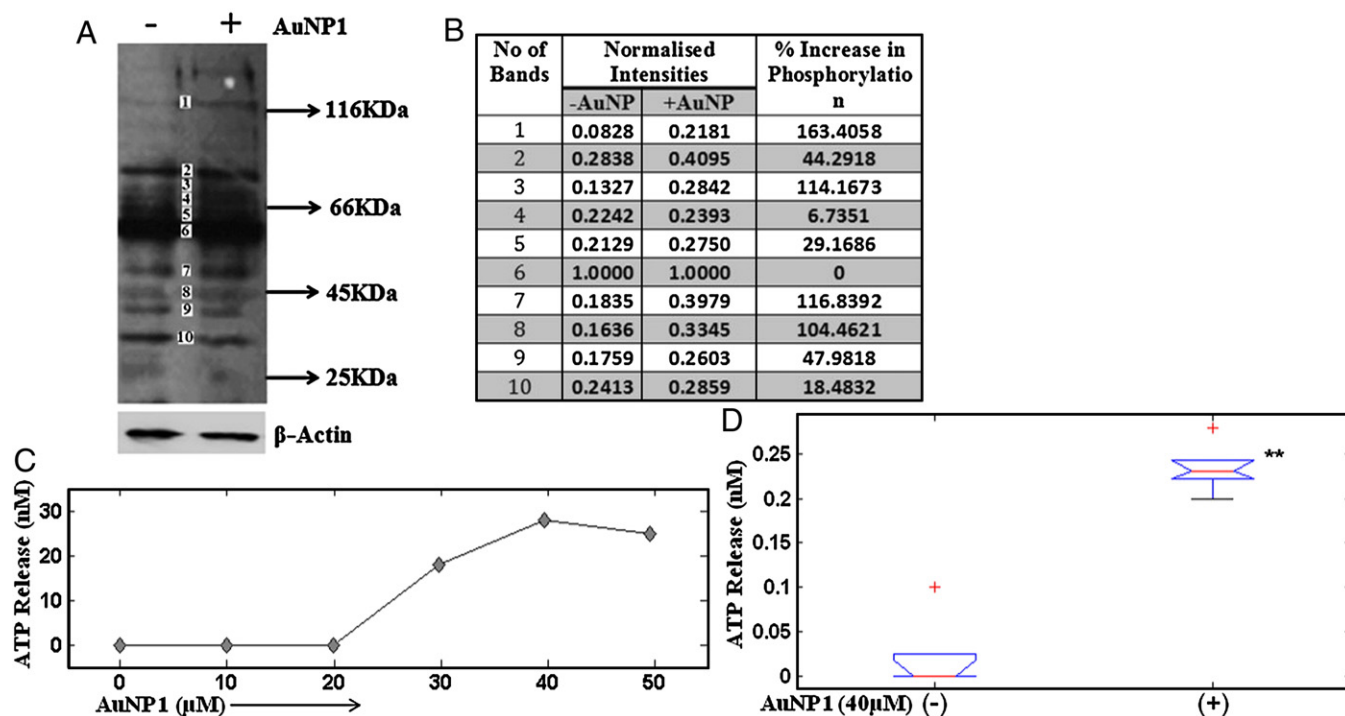


Figure 3. Platelet tyrosine phosphorylation and dense granule ATP release in the presence of AuNP. (A) represents the platelet tyrosine phosphorylation. Washed platelet tyrosine phosphorylation becomes increased in the presence of AuNP (40  $\mu$ M) in suspension condition.  $\beta$ -actin shows loading control. (B) provides the analysis of tyrosine phosphorylated protein bands and it shows that there is differential increase in individual bands and a 37% increase in the overall phosphorylation pattern. (C) represents ATP secretion kinetics with the increasing concentration of AuNP (from 0 - 50  $\mu$ M) in the presence of threshold concentration of ADP (0.4  $\mu$ M). Figure 3 (D) is the box plot representation of maximum ATP release (nM) in the presence and absence of AuNPs in five different healthy individuals and shows the ATP release is increased significantly ( $P$  value < 0.01) in the presence of AuNP (40  $\mu$ M).

40  $\mu$ M final concentration) induced aggregation are studied. The AuNP effect is described in the five respective panels. The panel marked with an arrow (Figure 2, A [iii]) corresponds to the critical NP-induced effect. The critical concentration has a distinctive feature. The steady state crosses a meta-stable aggregative state and shifts to a lower state of aggregation. We term this the de-aggregatory phase (see Figure 2, A [i]-[ii]), in which the stable steady state shows a lower value of percentage aggregation. Beyond the critical point (see Figure 2, A [iii]), there is a rapid jump to aggregative phase when there exists another steady state (see Figure 2, A [iv]-[v]) with higher aggregation value. Notably, the NP shows an insignificant pro-aggregatory effect in either of the two steady states but is most effective at the critical point when the stable profile switches from a de-aggregatory nature to an aggregatory nature. The difference in aggregation profile in Figure 2, A (iii) is evident from comparison with the profiles represented by the lighter (AuNP absent) and darker lines (AuNP present). The differences seen in Figure 2, A (i)-(ii) and (iii)-(iv) confirms the conjecture regarding the maximal sensitivity at the critical point. The window of ADP concentration at which the transition from the steady state occurs has subject dependence, with normal subjects showing a range (1.5 - 2  $\mu$ M). Figure 2, B illustrates the statistical nature of this individual dependence of critical behavior. The upper, middle and lower row (Figure 2), respectively, represents the subcritical, critical and higher-than-critical ADP concentration

of AuNP (40  $\mu$ M). The maximum aggregation and final aggregation values of 10 individuals of each group (subcritical, critical and higher-than-critical) are plotted, with an error bar (Figure 2, B). As expected, the critical concentration is marked by the maximal difference in aggregation before and after AuNP treatment, and  $P$  value is much lower than 0.01. In the Figure (+) and (-) in a given case represents the presence and absence of AuNP (40  $\mu$ M).

#### AuNP-induced dense granule ATP release and tyrosine phosphorylation

Figure 3, A illustrates the AuNP-induced enhancement of the phosphorylation pattern. The intensity values of the respective bands (Figure 3, B) increased in the presence of AuNP1. Different bands show different levels of activation. The mean enhancement of tyrosine phosphorylation considering all the bands is on the order of 37%.

Additional molecular evidence of the modulation of platelet signaling by AuNP is shown using the release reaction. Figure 3, C shows that each individual has the ability to increase platelet-dense granule release in a concentration-dependent manner. With the increase in the concentration of AuNP, the ATP release reaction is also increased from 0 to 28 nM. Beyond the 40  $\mu$ M concentration of AuNP1, the granule release saturates. Figure 3, D shows the statistical significance of ATP release from the dense granule in five healthy individuals in the absence and



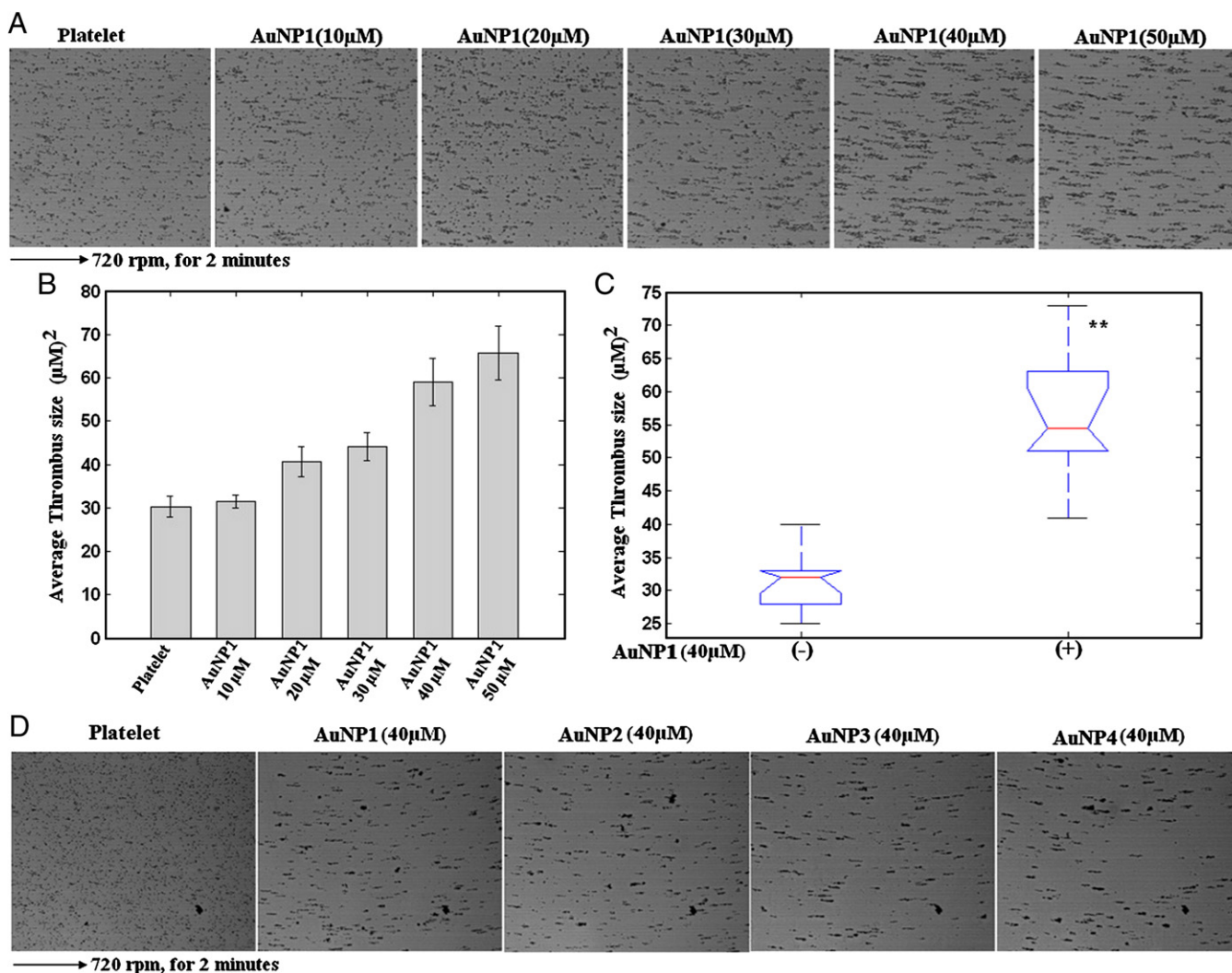


Figure 4. Dose dependency and size dependency on AuNPs in platelet aggregation in adhered condition. **(A)** represents bright field microscopic image of platelet aggregation in protein coated surface (fibrinogen and von Willebrand factor) in the presence of an increasing order of concentration of AuNPs (concentration ranging from 0 - 50  $\mu\text{M}$ ). The images are taken in 20 $\times$  magnification. **(B)** represents the bar diagram representation of the thrombus volume ( $\mu\text{m}^3$ ) calculated from the microscopic images. **(C)** shows the box plot representation of platelet aggregation formation in the presence of AuNPs (40  $\mu\text{M}$ ) in twelve healthy individuals, and the  $P$  value is  $< 0.01$ . **(D)** represents the size dependency of AuNPs. It shows the microscopic image of platelet aggregation (20  $\times$  magnification) with AuNP1, AuNP2, AuNP3, and AuNP4 with final concentration 40  $\mu\text{M}$ .

presence of 40  $\mu\text{M}$  AuNP1 ( $\sim 20$  nm). As expected there is significant change, and the  $P$  value is lower than 0.01.

#### Dose and size dependency of AuNP for adhered platelets

The critical behavior is further reflected in cone and plate imaging technique (described in the [Supplementary Section](#)) shown in [Figure 4](#). One important difference between cone and plate studies with suspension-based aggregometric studies (see Methods section, described in the [Supplementary Section](#)) is that AuNPs alter the platelet-aggregation profile even in absence of any agonist (ADP). The shear force applied in this platelet imaging technique (associated with the cone and plate assay) however imparts a residual activation in the platelets. The plate provided by the Diamed impact-R is coated with fibrinogen and vWF. With the increasing dose of AuNPs from 0 to 50  $\mu\text{M}$ , platelet aggregation increases ([Figure 4, A](#)). The thrombus

volume ( $\mu\text{m}^2$ ) has been statistically analyzed and plotted with an error bar by averaging out the pictures grabbed 7 times ( $n = 7$ ) for each run ([Figure 4, B](#)). AuNP (40  $\mu\text{M}$ ) induced aggregation was measured in twelve normal individuals, and plotted as a box plot with an error bar, which shows a significant change of the thrombus volume,  $P$  value  $< 0.01$  ([Figure 4, C](#)). Interestingly, there is no significant difference between the effect of increased size of NPs (AuNP 1-4) with the same concentration (40  $\mu\text{M}$ ) ([Figure 4, D](#)).

#### Fluorescence studies on NP uptake and scanning electron microscopy of AuNP-activated platelets

[Figure 5, A](#) shows the quenching curve for the 18 and 68 nm AuNP (see [Supplementary Section](#) for details). It is clear that the  $K_D$  value of an 18 nm particle ( $3.63 \times 10^3$ ) is slightly higher than that of the 68 nm particle ( $2.4 \times 10^3$ ). The

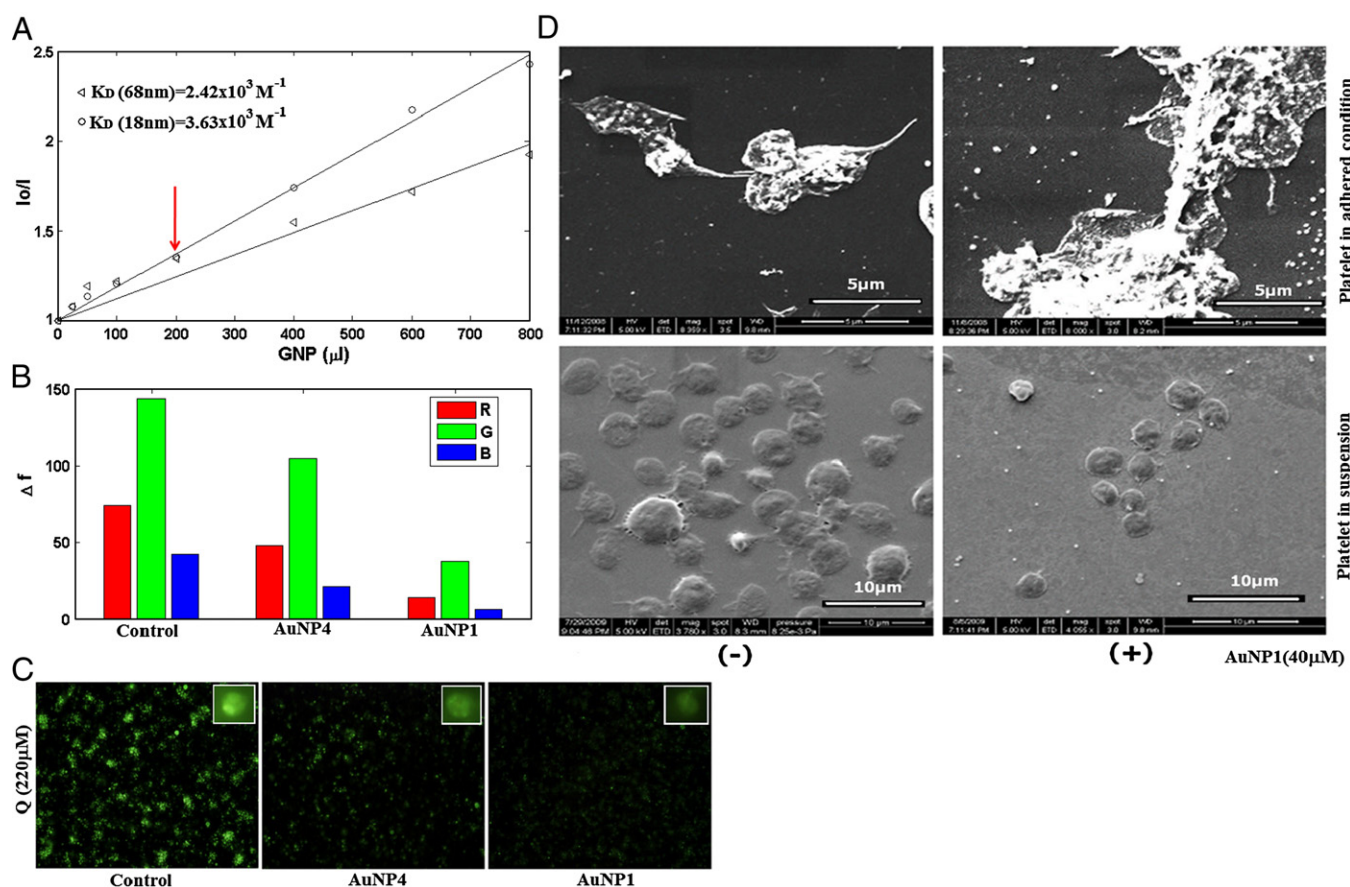


Figure 5. Fluorescence image of size-dependent uptake of AuNPs by platelets and scanning electron microscopy of AuNP-activated platelets. (A) represents the Stern-Volmer plot of quenching of Quinacrine hydrochloride by AuNP1 (18 nm) and AuNP4 (68 nm) [ $1 \mu$ l of AuNP =  $0.496 \mu$ M]. (B) Histogram of fluorescence intensities of the respective color planes of control (only Q), AuNP1 and AuNP4. (C) Fluorescence image of the control, AuNP1 and AuNP4 in 20 $\times$  magnification and inset showing the 100 $\times$  image of individual platelets. (D) Scanning electron microscopic image of platelet absence (-) and presence (+) of AuNP (40  $\mu$ M) in adhered condition and suspension. The upper panels represent the platelets adhered to a protein coated on the plate surface, whereas the lower panels show platelets suspended in Hepes buffer at pH 7.4.

observed difference in quenching (Figure 5, B and C) in the control (AuNP absent), 68 nm and 20 nm AuNP, is significant. As we have chosen a quencher (AuNP) concentration at which the fluorescence intensity of the two NPs are almost the same (see arrow in Figure 5, A), the high level of intensity reduction (one third times in the 68 nm particle and one fifth in the 20 nm particle) obviously implies a higher uptake of the smaller NP. The green plane data obtained from the microscopic image reflects fluorescence changes around the emission wavelength (500 nm).

The scanning electron microscopic studies (shown in Figure 5, D) compare the AuNP1 (40  $\mu$ M) induced activation of platelets in suspended and adhered states. In the presence of frictional force in the adhered condition (upper panel of Figure 5, D), there is a significant alteration in platelet morphology. AuNPs remain neutral when platelets are in suspension and no agonists are present (lower panel of Figure 5, D). That is clearly reverse in the case of adhered platelets. Images were captured under different magnifications (indicated in the figure legend) in the range 4000 $\times$  to 8000 $\times$ .

#### Individual variability of nano-response

As shown in Figure 6, the AuNP-induced response to NPs shows an individual dependent variation. The nanosafety measure (NSM) is expressed by the difference of percent aggregation in the presence and absence of NPs at threshold ADP concentrations. The measure expresses the risk of a given individual to exposure to a nano-drug as the individual (marked (i) in the Figure 6) is most prone to a NP-induced pro-aggregatory effect. The opposite is the case for the individual marked (iii).

#### Discussion

The chemically inert nature of gold and the high permeability of AuNPs in cells makes this NP an attractive drug-delivery agent.<sup>2,27</sup> The pro-aggregatory effect of AuNPs on platelets<sup>11,12</sup> thus needs a critical analysis. It is also reported that polymer-based NP-induced platelet aggregation shows size dependence.<sup>28</sup> The pro-aggregatory effect is, however, not universal, as a recent report shows that antiplatelet effects can be observed with silver

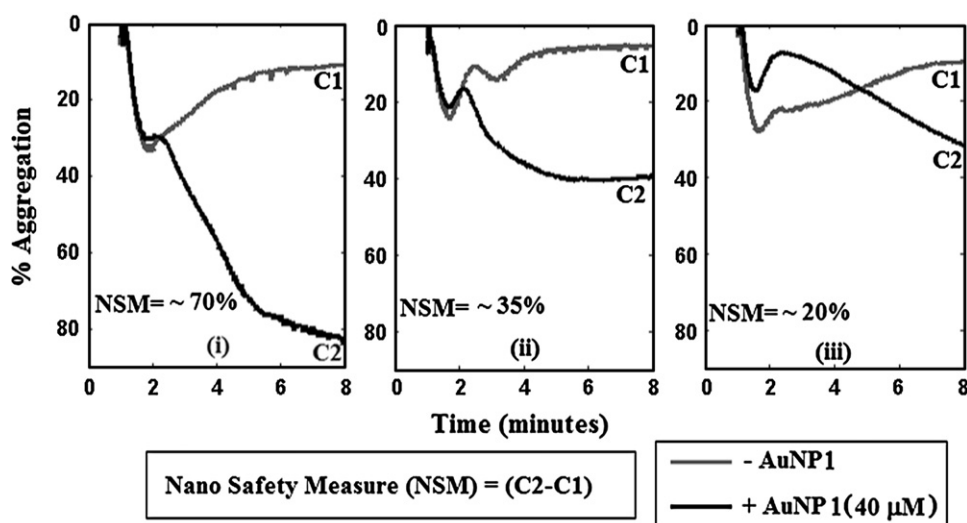


Figure 6. Inter-individual variability of AuNP induced platelet aggregation. The figure illustrates how the AuNP affects the aggregatory behavior of the platelets at the critical ADP concentration that causes transition from de-aggregatory to aggregatory behavior. The individuals (i-iii) shows a gradually decreasing risk as evident from a gradual decrease of NSM as explained in the text (Results). The respective NSM values are 70%, 35% and 20%.

NPs.<sup>29</sup> Similarly, the earlier report by Radomski et al indicated that among different carbon NPs, C60 did not induce any aggregation.<sup>13</sup> Therefore, the shape, surface and the constituent material dependence of the NPs play key roles in dictating the thrombotic response. The previous observation that AuNPs have pro-aggregatory effects in the presence of a critical dose of an agonist raises questions that warrant further investigation.

The size dependence of the NPs in platelets deserves special attention. Suspended- condition platelet aggregation was carried out with different sizes of AuNPs and also with different doses of the same (see Figure 1, A). The AuNPs of smaller size (20 nm), with 40 μM final concentration, activates the platelets maximally (Supplementary Figure 1 and Supplementary Figure 2). This is remarkable, as in most of the earlier reports on the effects of different sizes of AuNPs, (e.g., on cancer cells) 50 to 60 nm is the optimum size for the cellular uptake.<sup>17,30</sup> In contrast, for platelets, AuNPs greater than 60 nm in size are practically inert (Figure 1). The mechanism of uptake of the AuNPs in platelets is therefore distinctively different from that operating in the cancer cells. The observed size dependence may be explained by AuNP transport through open an canaliculer system<sup>31</sup> in platelets. We have also observed that for AuNPs with different zeta potentials, when suspended in PPP, the potential ( $\zeta$ ) assumes a low value  $\sim -7.04$  mV irrespective of the initial value of the surface potential. The  $\zeta$  assumes  $-7.76$  mV,  $-7.28$  mV,  $-8.76$  mV,  $-7.99$  mV, for AuNP1, AuNP2, AuNP3 and AuNP4, respectively. Thus, the contribution of surface potential in the AuNP uptake is minimal in this particular case. The outcome, however, would differ if the NP surface is covalently conjugated with charged molecules.

To observe an aggregatory response, the incubation with AuNPs with the platelet before activation (by ADP) is required. The reverse order of addition (namely AuNP followed by ADP) is not effective in inducing any incremental platelet response.<sup>11</sup> The requirement of pre-incubation is possibly due to the finite

time required for such entry through the open canaliculer system,<sup>31</sup> and this needs further study.

A frictional shear in an adhered condition can also lead to platelet aggregation by AuNPs without an agonist (see Figures 4 and 5, D). In the adhered state, the platelets are forced to float on a solid surface (mimicking a wound or a rupture in a blood vessel, i.e., exposed to the subendothelial extracellular matrix), and the effective frictional force is higher than what is present in the suspended condition. This is evident from the platelet shape change (see Figure 5, D). Thus the frictional force alone acts as a mild activator (like the critical ADP dose effect in suspension). The top and bottom row of (Figure 5, D) may be compared for this purpose. In adhered state platelet aggregation, in contrast to the suspended condition, is neutral to AuNP size. The adhered state of platelets thus deserves special attention. Unlike the suspended condition, the adhered state may follow an indirect route for NP-induced activation by an additional frictional force at the adhering interface. Furthermore, AuNP uptake by the platelets may be enhanced due to the lower dimensionality of the diffusion process (as it is known that in the case of low dimension diffusion, uptake is faster). Taking these two aspects into consideration, we may explain the characteristic of size response in adhered and suspended conditions.

RGDS, one of the major blockers of GpIIb/IIIa,<sup>32</sup> effectively blocks NP-induced platelet aggregation. However, at the molecular level RGDS is unable to block the enhancement of CD62P expression (Supplementary Section Figure 5). This implies that AuNP-induced platelet response is not due to any physicochemical cluster formation or nonspecific hydrophobic collapse between platelets and NPs and is mediated by the intracellular signalling in platelets.

The increased level of tyrosine phosphorylation is a good marker of platelet activation.<sup>25,33</sup> Image analysis of the immunoblot (Figure 3, B) indicates an increase of phosphorylation by



~ 37% in the presence of AuNP1. Different phosphorylated proteins (Figure 3, B) show a characteristic increase in expression level, indicating that the AuNP itself can be responsible for this mild activation. A detailed proteomic profile would reveal the AuNP-specific alteration in the platelet signalling circuit.

This study further reveals the mechanism of AuNP-induced prothrombotic effect. In washed platelets, the NP does not induce any aggregation, though surface CD62P expression is increased (Figure 1, B & Supplementary Section Figure 4). Platelet activation by alpha granule release is also implied.<sup>34,35</sup> Again, with an increase of the AuNP dose, ATP release from platelet-dense granules also increases (Figure 3, C and D). In the presence of apyrase, a phosphatase that scavenges ADP, the AuNP fails to cause aggregation in the suspended<sup>11</sup> or adhered condition (Supplementary Section Figure 3). Similarly, the inhibition of a AuNP-mediated induction of pro-aggregatory effect is observed in presence of the P2Y12 blocker Clopidogrel.<sup>11</sup> In the case of apyrase and/or Clopidogrel, though the granule release is not inhibited, agonists released from the granules fail to exert additional activation and thus AuNP-induced aggregation is inhibited. Moreover, an AuNP-induced aggregation pattern (see Figure 2, A [iii]) carries a similar signature observed in release reaction.<sup>36</sup> Therefore, it is suggested that AuNP-induced platelet activation is possibly due to a mild alteration of granule release, which under critical conditions can lead to aggregation.<sup>37,38</sup>

Until now, there is no robust and simple study regarding the NP entry into the cell. The TEM study of NP entry is also to some extent dependent on the field selection. Therefore, we developed a simple uptake experiment using the fluorescent drug (dye) Q (alternatively called mepacrine), the method being detailed in the Supplementary Section. In platelets the fluorescence from the dye is primarily a reflection of the binding with the platelet granules. This is the first report describing the quenching of Q by AuNP (Figure 5, A). As indicated earlier, the observed difference of fluorescence intensity in the presence of AuNP1 and AuNP4 could not be explained by size-dependent differences of quenching, because the extent of quenching at the concentration used is similar for the AuNP pair. Higher uptake of the smaller NPs remains the sole explanation of this multifold difference. The method described here may be of some general interest as it can be employed to study AuNP uptake in any Q-permeable cell.

Last, the one important question may be how activation and aggregation are coupled or decoupled at the molecular level. With a mild perturbation (e.g., NP-induced activation) there is overexpression of the platelet CD62P level, but this is accompanied by insignificant change (either very mild increase or in most cases, a decrease) in the GpIIb/IIIa expression (Supplementary Section Figure 4). Therefore, no positive correlation exists between activation and aggregation as long as the activation is below a critical level. Beyond this point of activation, however, there is a clear dependence of the GpIIb/IIIa expression on the CD62P level.<sup>39</sup> The NP context thus raises an important question: What is the threshold level of activation that would lead to aggregation?

Based on this study, we can develop strategies to formulate safer nano-drugs. It may be important to alter the formulation of

nano-drugs made for cancer applications and applications in diseases related to platelet disorders. Whereas in cancer cells ~50 nm size is most effective (cytotoxic and high penetrative nature), this size is apparently neutral to the thrombotic pathway. On the other hand, for a patient with a bleeding disorder, the presence of smaller size particle may be more useful as drug-delivery agent, because additionally it can be used as a hemostatic controller of bleeding. In the safety context, any open wound inside the body (where subendothelial ECM is exposed) would make the nano-based drug delivery unsafe; the pro-aggregatory effect of NPs may cause loss of homeostatic balance in such conditions. Our observation further indicates that this shortcoming of nano-drugs can be overcome by combination drugs in which inhibitors like Clopidogrel or Reopro (the same as RGDS) are present.

The platelets, in the presence of ADP, shows a multistable behavior.<sup>36</sup> Such multistable behavior is reported in many cell biological contexts.<sup>40,41</sup> For human platelets however, such behaviour is specific for ADP and not observed in the case of other agonists like epinephrine, collagen, etc. The threshold concentration of ADP at which the steady state switches from the de-aggregatory profile to aggregatory profile is specific to the prognostic condition of the patients. As AuNPs are shown to be most effective at this threshold regime, the NP response study may serve as an important measure for thrombotic risk and nano-safety (as illustrated in Figure 6). The extent of NP-induced enhancement of aggregation at the critical point (critical ADP concentration) would suggest how susceptible the platelet is to a basal level of activation and at what level of such activity the platelet would transit to the aggregatory phase. At the same time, irrespective of aggregation variation between individuals, if some NPs show constitutive higher NSM (Figure 6), special precautions should be taken before their administration as a drug or drug carrier.

## Appendix A. Supplementary data

Supplementary data associated with this article can be found, in the online version, at doi:10.1016/j.nano.2011.01.007.

## References

1. Patra HK, Banerjee S, Chaudhuri U, et al. Cell selective response to gold nanoparticle. *Nanomedicine* 2007;3:11–119.
2. Han G, Ghosh P, De M, Rotello VM. Drug and gene delivery using gold nanoparticles. *Nanobiotechnology* 2007;3:40–5.
3. Geys J, Nemmar A, Verbeken E, et al. Acute toxicity and prothrombotic effects of quantum dots: impact of surface charge. *Environ Health Perspect* 2008;116:1607–13.
4. Oberdörster G, Stone V, Donaldson K. Toxicology of nanoparticles: A historical perspective. *Nanotoxicology* 2007;1:2–25.
5. Morris JB, Olzinski AR, Bernard RE, et al. 38 MAPK inhibition reduces aortic ultrasmall superparamagnetic iron oxide uptake in a mouse model of atherosclerosis: MRI assessment. *Arterioscler Thromb Vasc Biol* 2008;28:265–71.
6. Rodvien R, Mielke CH. Role of platelets in hemostasis and thrombosis. *West J Med* 1976;125:181–6.
7. Kichler TS. Platelet biology – An overview. *Transfus Altern Transfus Med* 2006;8:79–85.



8. Mazzucato M, Cozzi MR, Pradella P, Perissinotto D, Malmstro MA, Morgelin MM, et al. Vascular PG-M/versican variants promote platelet adhesion at low shear rates and cooperate with collagens to induce aggregation. *Arterioscler Thromb Vasc Biol* 2008;28:265-71.
9. Willoughby S, Holmes A, Loscalzo J. Platelets and cardiovascular disease. *Eur J Cardiovasc Nurs* 2002;1:273-88.
10. Tendra M, Wojakowski W. Role of antiplatelet drugs in the prevention of cardiovascular events. *Thromb Res* 2003;110:355-9.
11. Deb S, Chatterjee M, Bhattacharya J, Lahiri P, Chaudhuri U, Pal Choudhuri S, et al. Role of purinergic receptors in platelet-nanoparticle interactions. *Nanotoxicology* 2007;1:93-103.
12. Akchurin GG, Akchwin GG, Ivanovi AN, Kirichuk VF, Terentyuk GS, Khlebtsov BN, et al. Influence of gold nanoparticles on platelets functional activity in vitro. In: Tuan Vo-Dinh V, Lakowicz JR, editors. *Plasmonics in Biology and Medicine*, Vol. 6869. Bellingham, WA: SPIE; 2008. doi:10.1117/12.765076.
13. Radomski A, Jurasz P, Alonso-Escolano D, Drews M, Morandi M, Malinski T, Radomski MW. Nanoparticle-induced platelet aggregation and vascular thrombosis. *Br J Pharmacol* 2005;146:882-93.
14. Lu SH, Tun MHN, Mei ZJ, Chia GH, Lim X, Sow CH. Improved hydrophobicity of carbon nanotube arrays with micropatterning. *Langmuir* 2009;25:12806-11.
15. Ghosh P, Han G, De M, Kim CK, Rotello VM. Gold nanoparticles in delivery applications. *Adv Drug Deliv Rev* 2008;60:1307-15.
16. Huff TB, Tong L, Zhao Y, Hansen MN, Cheng JX, Wei A. Hyperthermic effects of gold nanorods on tumor cells. *Nanomedicine* 2007;2:125-32.
17. Arnida Malugin A, Ghandehari H. Cellular uptake and toxicity of gold nanoparticles in prostate cancer cells: a comparative study of rods and spheres. *J Appl Toxicol* 2010;30:212-7.
18. Singha S, Datta H, Dasgupta AK. Size dependent chaperon properties of gold nanoparticles. *J Nanosci Nanotechnol* 2010;10:826-32.
19. Born GV. Aggregation of blood platelets by adenosine diphosphate and its reversal. *Nature* 1962;194:927-9.
20. Higashi T, Isomoto A, Tyuma I, Kakishita E, Uomoto M, Nagai K. Quantitative and continuous analysis of ATP release from blood platelets with firefly luciferase luminescence. *Thromb Haemos* 1985; 53:65-69.
21. Panzer S, Eichelberger B, Koren D, Kaufmann K, Male C. Monitoring survival and function of transfused platelets in Bernard-Soulier syndrome by flow cytometry and a cone and plate(let) analyzer (Impact-R). *Transfusion* 2007;47:103-6.
22. Ray T, Maity P C, Banerjee S, Deb S, Dasgupta A K, Sarkar S, et al. Vitamin C prevents cigarette smoke induced atherosclerosis in guinea pig model. *J Atheroscler Thromb* 2010 (in press).
23. Zilla P, Fasol R, Hammerle A, Yildiz S, Kadletz M, Laufer G, Wollenek G, Seitelberger R, Deutsch M. Scanning electron microscopy of circulating platelets reveals new aspects of platelet alteration during cardiopulmonary bypass. *Tex Heart Inst J* 1987;14:13-21.
24. Walkowiak B, Kralisz U, Michalec L, Majewska E, Kiewicz WK, Ligocka A, et al. Comparison of platelet aggregability and P-selectin surface expression on platelets isolated by different methods. *Thromb Res* 2000;99:495-502.
25. Fälker K, Lange D, Presek P. P2Y<sub>12</sub> ADP receptor-dependent tyrosine phosphorylation of proteins of 27 and 31 kDa in thrombin-stimulated human platelets. *Thromb Haemost* 2005;93:880-8.
26. Michelson AD. Flow cytometry. A clinical test of platelet function. *Blood* 1996;87:4925-36.
27. Mandal D, Maran A, Yaszemski MJ, Bolander ME, Sarkar G. Uptake of gold nanoparticles directly cross-linked with carrier peptides by osteosarcoma cells. *J Mater Sci Mater Med* 2009;20:347-50.
28. Mayer A, Vadon M, Rinner B, Novak A, Wintersteiger R, Fröhlich E. The role of nanoparticle size in hemocompatibility. *Toxicology* 2009;258:139-47.
29. Shrivastava S, Bera T, K. Singh S, Singh G, Ramachandrarao P, Dash D. Characterization of antiplatelet properties of silver nanoparticles. *ACS Nano* 2009; 3:1357-64.
30. Chithrani BD, Ghazani AA, Chan WC. Determining the size and shape dependence of gold nanoparticle uptake into mammalian cells. *Nano Letter* 2006;6:662-8.
31. White JG. Platelets are coverocytes, not phagocytes: Uptake of bacteria involves channels of the open canalicular system. *Platelets* 2005;16:121-31.
32. Basani RB, D'Andrea G, Mitra N, Vilaire G, Richberg M, Kowalska MA, et al. RGD-containing peptides inhibit fibrinogen binding to platelet alpha(IIb)beta3 by inducing an allosteric change in the amino-terminal portion of alpha(IIb). *J Biol Chem* 2001;276:13975-81.
33. Golden A, Brugge JS, Shattil SJ. Role of platelet membrane glycoprotein IIb-IIIa in agonist-induced tyrosine phosphorylation of platelet proteins. *J Cell Biol* 1990;111:3117-27.
34. Harrison P, Cramer EM. Platelet alpha-granules. *Blood Rev* 1993;7: 52-62.
35. Taylor ML, Misso NL, Stewart GA, Thompson PJ. Differential expression of platelet activation markers in aspirin-sensitive asthmatics and normal subjects. *Clin Exp Allergy* 1996;26:202-15.
36. Laffan MA, Manning RA. Investigation of hemostasis. In: Lewis SM, Bain BJ, Bates I, editors. *Practical Haematology*. 9th ed. London, UK: Harcourt Publishers Limited; 2001. p. 339-90.
37. Daniel JL, Dangelmaier C, Jin J, Ashby B, Smith JB, Kunapuli SP. Molecular basis for ADP-induced platelet activation. *J Biol Chem* 1998;273:2024-9.
38. Huang PY, Hellums JD. Aggregation and disaggregation kinetics of human blood platelets Part II. Shear-induced platelet aggregation. *Biophys J* 1993;65:344-53.
39. Merten M, Thiagarajan P. P-selectin expression on platelets determines size and stability of platelet aggregates. *Circulation* 2000;102:1931-6.
40. Dubnau D, Losick R. Bistability in bacteria. *Mol Microbiol* 2006;61:564-72.
41. Ozbudak EM, Thattai M, Lim HN, Shraiman BI, Oudenaarden AV. Multistability in the lactose utilization network of *Escherichia coli*. *Nature* 2004;427:737-40.